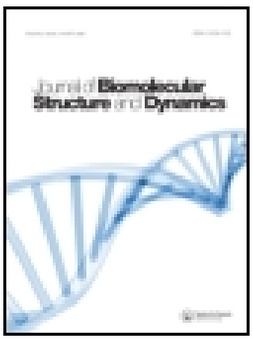

Taylor & Francis
Taylor & Francis Group

Journal of Biomolecular Structure and Dynamics

ISSN: (Print) (Online) Journal homepage: https://www.tandfonline.com/loi/tbsd20

Identification of zebrafish fumarate hydratase active site by molecular docking and simulation studies

Venkatasubramanian Hemagowri , Velanganni Selvaraj , R. Jesu Jaya Sudan , Sudandiradoss Chinnappan , Anbalagan Bhuvan & Kirankumar Santhakumar

To cite this article: Venkatasubramanian Hemagowri , Velanganni Selvaraj , R. Jesu Jaya Sudan , Sudandiradoss Chinnappan , Anbalagan Bhuvan & Kirankumar Santhakumar (2020): Identification of zebrafish fumarate hydratase active site by molecular docking and simulation studies, Journal of Biomolecular Structure and Dynamics, DOI: 10.1080/07391102.2020.1824812

To link to this article: https://doi.org/10.1080/07391102.2020.1824812

Published online: 24 Sep 2020.

JOURNAL OF BIOMOLECULAR STRUCTURE AND DYNAMICS
https://doi.org/10.1080/07391102.2020.1824812

Identification of zebrafish fumarate hydratase active site by molecular docking and simulation studies

Venkatasubramanian Hemagowri[a], Velanganni Selvaraj[a], R. Jesu Jaya Sudan[b], Sudandiradoss Chinnappan[c], Anbalagan Bhuvan[a] and Kirankumar Santhakumar[a]

[a]Zebrafish Genetics Laboratory, Department of Genetic Engineering, School of Bioengineering, SRM Institute of Science and Technology, Kattankulathur, Chengalpattu, Tamil Nadu, India; [b]Department of Biotechnology, Marudhar Kesari Jain College for Women, Vaniyambadi, Vellore, Tamil Nadu, India; [c]Division of Bioinformatics, VIT University, Vellore, Tamil Nadu, India

Communicated by Ramaswamy H. Sarma

ABSTRACT

Fumarate hydratase (FH), one of the members of TCA cycle, acts as a catalyte for the synthesis of malate from fumarate. FH has been proposed to play as a tumour suppressor leading to the pathogenicity of leiomyomas, renal cell carcinoma and paraganglioma. Mutations in the active site of FH lead to alteration in the protein structure. Similarly, binding of several chemical inhibitors to the active site also leads to the disruption of protein structural integrity thereby leading to protein dysfunction. Therefore, in order to address this mechanism leading to cancer, the binding efficiency of potential human FH inhibitor citrate to zebrafish fh has been extensively analysed in this study by molecular docking and simulation experiments followed by quantification of fumarate hydratase enzyme activity to validate and confirm the findings. Molecular docking revealed stronger interaction of zebrafish fh protein with inhibitor citrate when compared to natural substrate fumarate. Study on the dynamics of docked structures further confirmed that citrate was found to possess more binding affinity than fumarate. *In vitro* biochemical analysis also revealed concentration dependent potential inhibitory effect of citrate on zebrafish fh, thus confirming the findings of the *in-silico* experiments.

ARTICLE HISTORY
Received 29 May 2020
Accepted 12 September 2020

KEYWORDS
Fumarate hydratase; zebrafish; citrate; molecular dynamics; TCA cycle; *in silico*

Introduction

Fumarate hydratase (FH), also known as fumarase is a member of tricarboxylic acid (TCA) cycle enzymes which is highly conserved in its function from yeast to humans (Leshets et al., 2018; Mann & Woolf, 1930; Wu & Tzagoloff, 1987). FH catalyses a reversible process of hydratation that involves conversion of fumarate to malate. The enzyme FH exists in two isoforms, a mitochondrial form which is involved in TCA cycle and energy production and a cytosolic form is involved in both Non-homologous End Joining (NHEJ) and Homologous Recombination (HR) pathways of DNA repair system (Leshets et al., 2018; Yogev et al., 2010). Both mitochondrial and cytosolic isoforms are structurally identical except for the difference in the N-terminus region which differs between the isoforms (Doonan et al., 1984; O'Hare and Doonan, 1985). The FH protein is a homotetrameric protein with the molecular weight of 200 KDa. The 'active site' in the tetrameric structure is formed by the union of the amino acid residues Thr143-Thr147 and Ser186-Asn188 of chain A, amino acid residues Ser365-Glu378 from chain B and residues Thr234-His235 from chain C and this active site forming residues are found to be highly conserved across the kingdom (Bulku et al., 2018; Subasri et al., 2017; Woods et al., 1988). These residues are critical for binding of substrate fumarate to the active site and regulating the catalytic mechanism involved in the conversion of fumarate to malate (Picaud et al., 2011; Subasri et al., 2017)

The role of *FH* gene in HIF signalling and DNA repair mechanism provides insights into the role of *FH* as a tumour suppressor gene. Multiple Leiomyoma Consortium originally in 2002 proposed the tumour suppressor function in *FH* gene (Tomlinson et al., 2002). Later, two models have been proposed to understand the functional role of *fumarase* as a tumour suppressor gene in which the first model states that the loss of FH activity leads to accumulation of oncometabolite fumarate and stabilization of hypoxia-inducible factor −1 alpha (HIF-1α) and activation of genes involved in the cell proliferation (Isaacs et al., 2005; Pollard et al., 2005) while the second model proposes that the insufficient fumarate synthesis at the site of DNA repair due to loss of FH leads to defective DNA repair mechanism and thus leading to genomic instability (Jiang et al., 2015; Yogev et al., 2010). Both the models suggest that loss of functions of FH leads to tumourigenesis and hence FH is thought to play an important role in the tumourigenesis pathway. Further, different reports in humans also infer that pathogenic variants in this gene lead to predisposition of individuals to leiomyomas, renal cell carcinoma and paraganglioma (Alam et al., 2005; Castro-Vega et al., 2014; Leshets et al., 2018; Pollard et al., 2005; Schmidt

CONTACT Kirankumar Santhakumar kirankus@srmist.edu.in Zebrafish Genetics Laboratory, Department of Genetic Engineering, School of Bioengineering, SRM Institute of Science and Technology, Kattankulathur, Chengalpattu, Tamil Nadu, India

et al., 2019; Trpkov *et al*., 2016). A vast majority of mutations associated with different types of cancer like Multiple cutaneous and uterine leiomyomata (MCUL1) and Hereditary leiomyomatosis and renal cell carcinoma (HLRCC) are located in the active site region of FH which is highly conserved evolutionarily and these mutations are likely to disrupt the structural integrity and subsequently the loss of enzyme activity (Picaud et al., 2011). Therefore, it is evident that active site of FH serves as the hotspot region for tumour development.

In addition to the mutations observed in this region, several chemicals bind to the active site of FH and act as potential inhibitors of FH thus leading to loss of function of FH and thereby inducing tumourigenesis (Subasri et al., 2017; Teipel & Hill, 1968). In humans, molecular docking and molecular dynamics analysis have identified few potential competitive inhibitors of FH like citrate (a structural analogue of L-Malate) and pyromellitic acid (Subasri et al., 2017; Teipel & Hill, 1968). These studies show that the inhibitor molecules bind to the active site of the fh. In order to understand the tumour suppressor properties of zebrafish fumarate hydratase (fh) protein, it is very essential to study the mechanism of inhibition of fh by the characterized human FH inhibitors. In this study, protein structure of zebrafish fh was modelled and molecular docking, dynamics studies have been performed with its substrate fumarate and inhibitor citrate to identify the binding sites. Thus, this study will provide insights into the role of structure and function interrelationships in the pathogenesis of cancer.

Materials and methods

Prediction of zebrafish fumarate hydratase (FH) 3D protein structure

The amino acid sequence for zebrafish fh was retrieved from UniProt database with accession ID F1QWR4. The template structure was identified by sequence alignment method using NCBI BLAST server. The protein structure for zebrafish fh was then predicted by Modeller9v20 (Webb & Sali, 2016) software based on homology modelling approach. The generated protein model was validated for stereochemical properties using Procheck program.

Molecular docking of zebrafish fh with fumarate and citrate

Molecular docking of the zebrafish fumarate hydratase protein structure with its substrate fumarate and inhibitor citrate was performed using PatchDock (Schneidman-Duhovny et al., 2005) by targeted molecular docking approach where substrate binding sites for zebrafish fumarate hydratase were obtained from UniProt database and these sites were specified as binding sites for the ligands fumarate and citrate. The predicted protein structure was used as substrate and the ligand structures for fumarate and citrate were obtained from PubChem Database. Prior to docking the protein and ligand structures were prepared by adding hydrogens and removing any solvent molecules present in the crystallographic structure of the protein. The best docked pose was selected for further analyses.

Identification of interacting residues between zebrafish fh and substrates

The docked structures of zebrafish fh with fumarate and citrate were visualized using PyMOL visualization tool and the fh residues interacting with substrate fumarate and the inhibitor citrate were analysed using LIGPLOT v.4.5.3 (Laskowski & Swindells, 2011). The residues interacting with fumarate and citrate were compared.

Molecular dynamics simulation

MD simulation was carried out in explicit water using the force field gromos96 43a1 in Gromacs 4.5.3 package (Berendsen et al., 1995). The system was solvated using simple point charge (SPC) and electrically neutralized by adding ions. Steric clashes were removed by performing energy minimization using steepest descent algorithm and continued until it reached a tolerance of 1000 kJ/mol to remove steric conflicts implementing GROMOS96 43a1 force field. The entire system was heated from 0 to 300 K gradually over 100 ps using the NVT ensemble. The particle mesh Ewald method was used to treat long-range electrostatic forces and Lennard–Jones was set for Columbic interactions and the simulations performed. The LINCS algorithm was used to constrain bond lengths involving hydrogen. Finally, 10 ns MD simulations were conducted at 1 atm and 300 K under the NPT ensemble with a time step of 2 fs. The output files generated after the 10 ns simulation was analyzed by plotting in Xmgrace software.

Multiple sequence alignment and evolutionary conservation of interacting residues of zebrafish fh with other organisms

Multiple sequence alignment was performed using Clustal Omega by aligning the fumarate hydratase amino acid sequences of zebrafish (UniProt Accession No F1QWR4), mouse (*Mus musculus*), chimpanzee (*Pan troglodytes*) and human (*Homo sapiens*). ConSurf analysis was performed for the fumarate hydratase protein to identify the conservation of the functionally important amino acids interacting with the substrates fumarate and the inhibitor citrate using ConSurf Server (Ashkenazy et al., 2016).

Predicting the effect of mutations in the interacting residues

The corresponding interacting amino acid residues of human FH were identified and the occurrence of mutations in these residues was searched in the Ensembl data base. Then the identified SNPs were subjected to five different tools PANTHER (Mi et al., 2010), PolyPhen (Adzhubei et al., 2010), SIFT (Sim et al., 2012), PROVEAN (Choi & Chan, 2015) and SNPs & GO (Capriotti et al., 2013) to predict the effect of these mutations.

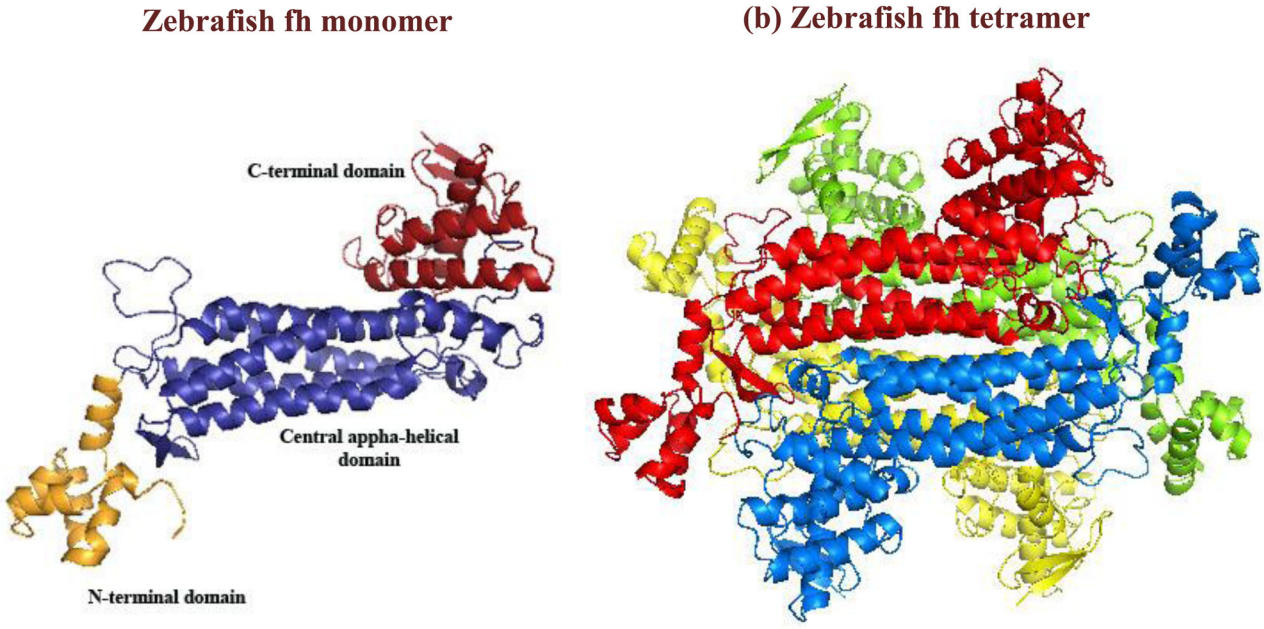

Figure 1. Zebrafish fh monomer (a) Red – C-terminal domain, Blue – Central alpha helical domain and Yellow- N-terminal domain, and (b) 3 D protein model (tetramer) generated by homology modelling.

Molecular docking of fumarate with native and mutated zebrafish fh protein structure

The predicted SNPs in human FH were incorporated in the zebrafish fh protein structure by mutating the corresponding amino acid residues in the zebrafish fh using the 'mutate' option in Swiss pdb viewer (Guex & Peitsch, 1997). The mutated protein structures were energy minimized using CHARMM software before docking. The ligand fumarate was docked with native as well as the mutated fh protein structure. The docked poses were subsequently analysed for the interactions in both the native and mutated fh-fumarate complexes.

Prediction and analysis of protein-ligand interactions using protein contacts atlas

Protein Contacts Atlas allows investigation of non-covalent interactions in addition to covalent interactions between protein and ligand in both native and mutated states (Kayikci et al., 2018). The docked complex for native and mutated proteins were given as input and processed in the home page of Protein Contacts Atlas. Different types of interaction plots like asteroid plot and scatter plot were obtained for each of the protein-ligand complex. The results were analysed, compared and interpreted.

In vitro biochemical assay for quantification of zebrafish fh activity

Fumarate hydratase enzyme activity was quantified by an *in vitro* biochemical assay (Patel et al., 1996). Briefly, zebrafish whole tissue was homogenized with phosphate buffer and the homogenate was centrifuged at 10,000 rpm. Then the supernatant was used for quantifying the fumarate hydratase enzyme activity. In a 3 ml cuvette, a reaction mix containing 30 mM KH_2PO_4, 0.1 mM EDTA and 5 mM L-Malic acid was added with 1.5ul of fish tissue sample. To demonstrate the inhibition activity of citrate, 5 mM and 10 mM sodium citrate was added to the sample and reaction mix and the OD was measured at 250 nm.

Results and discussion

Predicted protein structure for zebrafish fh

The tetramer structure of Zebrafish fumarate hydratase was modelled using human FH crystal structure as template (3E04), where the monomer and tetramer structures are shown in Figure 1. The predicted protein model showed a QMEAN (Qualitative Model Energy ANalysis) score of −0.87 and GMQE (Global Model Quality Estimation) score of 0.85. Ramachandran plot analysis for the predicted protein structure from PROCHECK server showed 93% of the residues in favourable region and 0.2% residues in the disallowed region. The residue properties for the protein structure showed zero bad contacts, suggesting to be a good model. The modelled zebrafish fh monomer structure was found to have a C-terminal domain, a central alpha helical domain and an N-terminal domain similar to that of human FH as reported in the study by Subasri et al. (2017) wherein human FH is found to be comprised of N-terminal domain formed by compact five-helix bundle which is flanked by 2 strands, a central helical domain composed of five alpha helices that are long and a C-terminal domain consisting of six short alpha helices.

Interaction between zebrafish fh and its substrate fumarate and inhibitor citrate

Docking studies zebrafish fh was carried out with its native substrate fumarate and inhibitor citrate using PatchDock. Binding site for the protein was obtained from Uniprot which revealed Thr146 as the binding site residue and hence this

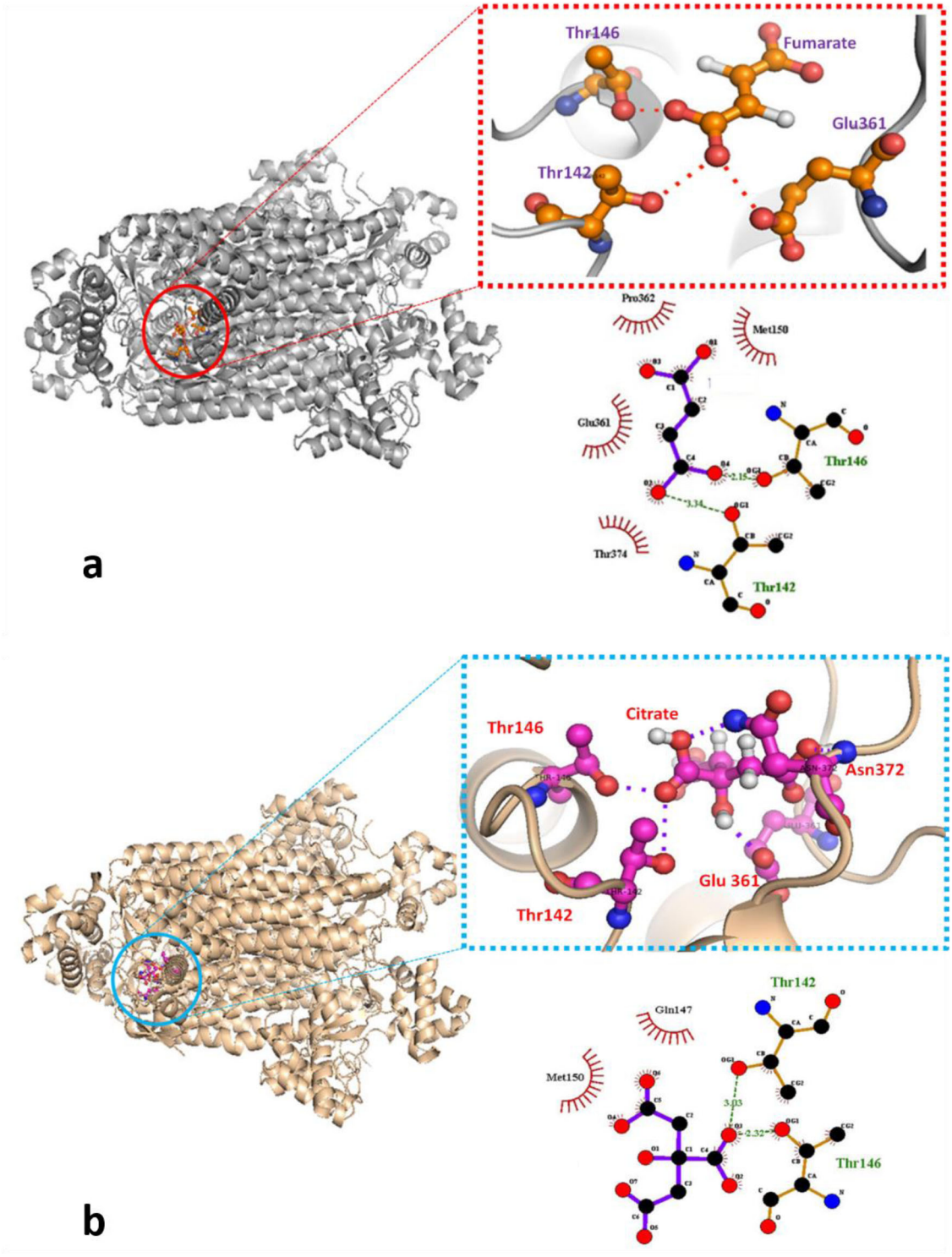

Figure 2. Predicted docking interactions of zebrafish fh with (a) fumarate and (b) citrate. The interaction between fumarate and fumarate hydratase residues T146, T142 and E361were predicted by Ligplot.

residue was used as the target site for docking. About 11 poses for fumarate and 20 poses for citrate were obtained through molecular docking. Ligplot analysis revealed the interactions of fumarate with zebrafish fh through the residues Thr146, Thr142 and Glu361 (Figure 2(a)), while citrate shows interactions with the residues Thr146, Thr142, Glu361 and Asn372 of zebrafish fh (Figure 2(b)). However, the top scoring binding poses for both the substrate fumarate and inhibitor citrate showed interaction with the binding site residue Thr146. In addition, the binding score of citrate was (2408) higher than that of fumarate (1916) indicating citrate has a better binding affinity than the substrate fumarate.

Conservation of residues in zebrafish fh interacting with fumarate and citrate

The active site residues of zebrafish fh Thr142, Thr146, Glu361 and Asn372 interacting with fumarate and citrate

were found to be highly conserved with FH amino acid sequences from other organisms like human, chimpanzee and mouse (Figure 3(a)). Further analysis using Consurf showed that all the four interacting amino acid residues were highly conserved with a predicted Consurf score of 9 (Figure 3(b)). A study in humans suggested that the 'active site' region of tetrameric FH structure was reported to be formed by the union of three regions constituting the amino acid residues Thr143-Thr147 and Ser186-Asn188 of chain A, amino acid residues Ser365-Glu378 from chain B and residues Thr234-His235 from chain D which is found to be highly conserved across the animal kingdom (Bulku et al., 2018; Subasri et al., 2017; Woods et al., 1988). These active site residues were reported to be critical for binding of substrate and regulating the catalytic mechanism (Picaud et al., 2011; Subasri et al., 2017). Similar to previous studies, the present study also suggests that the active residues T142, T146, E361 and N372 present in zebrafish fh, which are particularly involved in interaction with substrates like fumarate and citrate are highly conserved, thus indicating that active site in zebrafish fh also might be formed by the union of these regions.

Predicted list of mutations in the interacting residues

We searched the occurrence of mutations in the above-mentioned interacting residues and found five human nsSNPs in these residues. Analysis of these SNPs using five different tools revealed that the SNP variants obtained for all the residues were predicted to be pathogenic and it was observed that human variants T143L, T147A, E362Q, N373S and N373D were predicted as damaging or deleterious by at least one of the five tools (Table 1). Hence inhibiting fumarate hydratase with the inhibitor citrate may mimic the pathogenic conditions observed in patients having mutations in the interacting residues. In order to understand the role of these active site interacting residues, all the above mentioned nsSNPs were incorporated in to the native structure to model the corresponding mutated structures. The mutated structures were docked with the substrate fumarate and the binding efficacy of the substrate to fh both in native and mutated states were analysed.

Interaction of mutated zebrafish fh with fumarate

The native protein structure of zebrafish fh was mutated with the aminoacid residues corresponding to the above predicted SNPs in the human FH structure (Table 1). The docking analysis revealed that these mutated residues were not interacting with the substrate (fumarate) indicating that the mutations have altered the conformation of protein structure.

To further validate the results, all the five docked mutant fh-fumarate complexes were subjected to an interaction analysis using Protein Contacts Atlas (Figures 4 and 5). Figure 4 shows the non-covalent interaction of the substrate fumarate with its atomic neighbourhood in both native and mutated fh proteins. The analysis showed that the first line of contacts was different for the variants T142L, T146A and E361Q when compared to native fh protein. Further each of the mutated active site residue (Table 1) was selected to identify the alteration in the interaction of the mutated residue with their interacting residues (Figure 5). These results revealed that the pattern of hydrogen bond and non-covalent interactions of the mutated active site residues with fumarate was altered in all the mutated structures (T142L, T146A, E361Q, N372D and N372S). There was no hydrogen bond as well as non-covalent interactions between the mutated residues T142L, T146A and E361Q and the substrate fumarate. Although there was non-covalent interactions of the mutated residues N372D and N372S with fumarate, the number of atomic contacts were less compared to the native amino acid and this is indicated by the reduced size of the node in the asteroid plot (Kayikci et al., 2018). However, hydrogen bonds were not formed with fumarate in these two mutated forms (Figure 5 d (vi) and e(iii)).

The closeness of selected residue with the other residues provides information about the protein stability. The closeness of the native and the mutated residues with their neighbouring residues were analysed and the results are represented as a scatter plot (Figure. 5). The scatter plot also provides information on the solvent accessibility area of each amino acid along with the degree of amino acid present in the protein structure. It was observed that T146A, N372D and N372S were not involved in close contacts with other residues but although T142L and E361Q were found to be involved in contacts, they did not interact with the substrate fumarate, suggesting a possible change in the protein conformation. The degree and solvent accessibility of the mutated amino acids T146A, N372D and N372S were also found to be altered.

These observations suggest that the interacting active site residues T142, T146, E361 and N372 are crucial for binding of the substrate fumarate. A similar study on human FH by Subasri et al. (2017) suggested that mutation in one of the active site residues H235N of human FH led to a change in the protein structure conformation and further alterations in binding ability of fumarase inhibitors citrate and pyromalletic acid to FH (Subasri et al., 2017). Consistent with the earlier studies, the observations in the present study also indicates that mutation in all the four of the active site residues have led to a conformational change in the protein structure and therefore leading to inability of the natural substrate fumarate to bind to zebrafish fh.

Closeness, betweeness, degree and the solvated area for the native (a-d (ii)) and the corresponding mutated (a-d (v) and e (ii)) active site residues are given. The interaction of fumarate with the native (a-d (iii)) and the corresponding mutated (a-d (vi) and e (iii)) active site residues are visualized after docking.

Molecular dynamics simulation- Root mean square deviation (RMSD)

Molecular Dynamics simulation is currently an advanced approach to study the behaviour of macromolecules in the

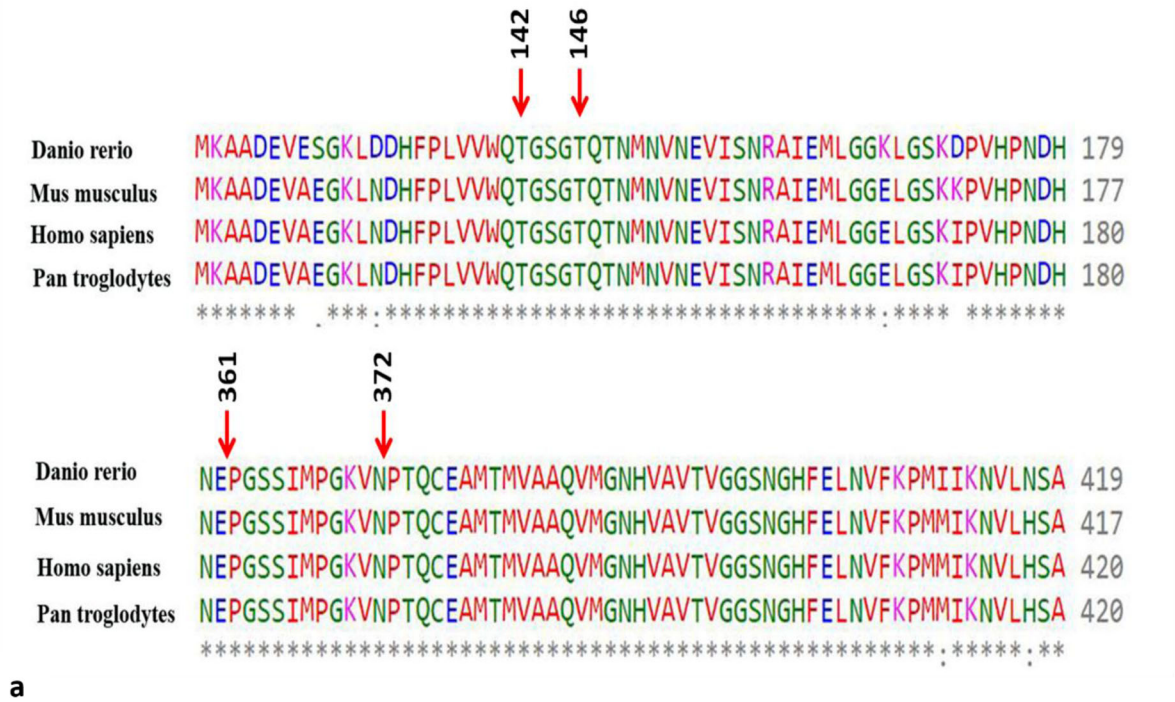

a

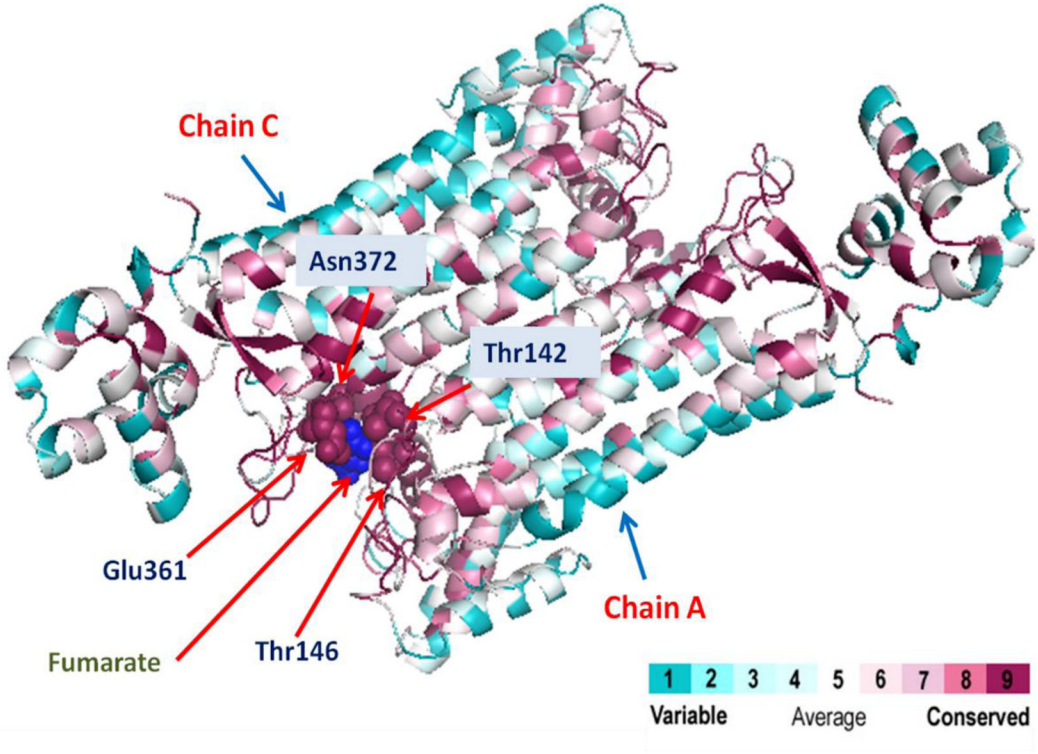

b

Figure 3. (a) Multiple sequence alignment of fumarate hydratase protein sequence from different species shows that the residues interacting with fumarate and citrate are conserved, (b) Consurf evolutionary analysis of the interacting residues T142, T146, E361 and N372.

Table 1. List of mutations present in the interacting residues.

AA Residues	PANTHER	Polyphen-2	SIFT	PROVEAN	SNP&GO
T143L	Probably damaging	Damaging	Damaging	Deleterious	Disease
T147A	Probably damaging	Damaging	Damaging	Deleterious	Disease
E362Q	Probably damaging	Damaging	Damaging	Deleterious	Neutral
N373S	Probably damaging	Damaging	Damaging	Tolerated	Disease
N373D	Probably damaging	Damaging	Damaging	Deleterious	Disease

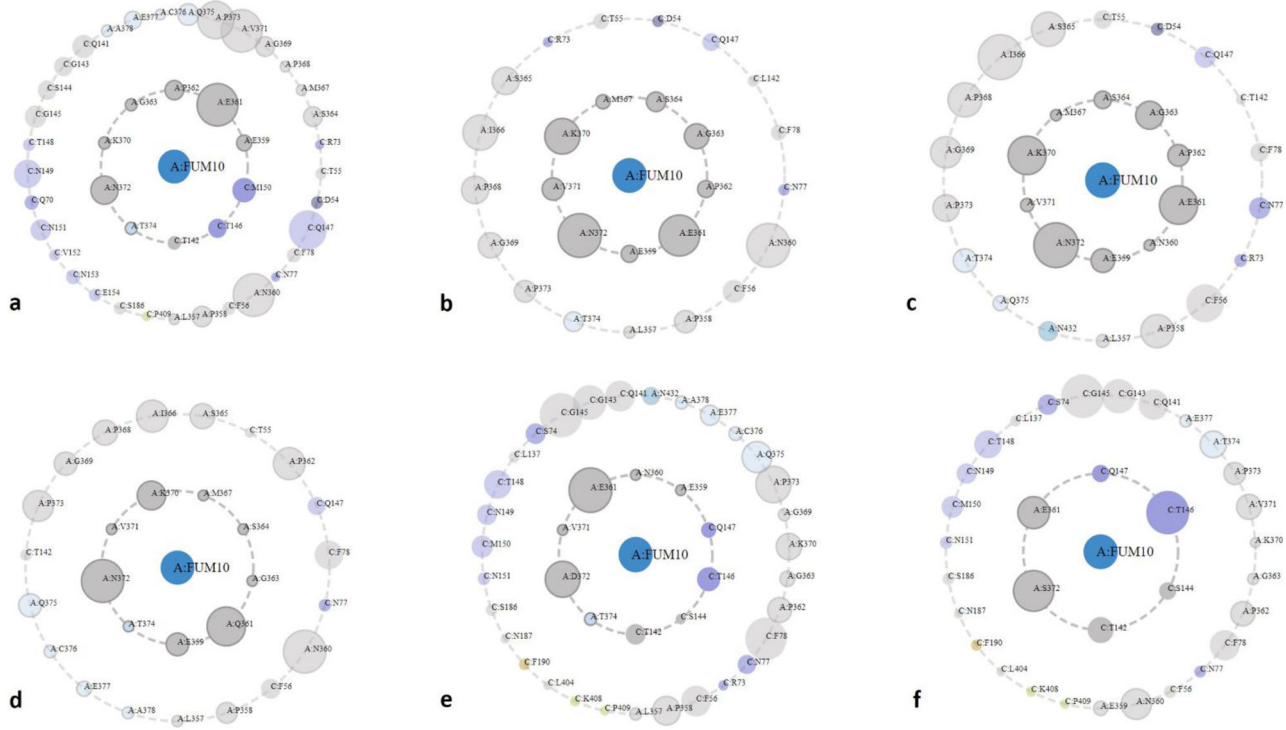

Figure 4. Molecular docking analysis showing the interaction of fumarate with native fumarate hydratase and different mutated forms of fumarate hydratase, (a) Native fh, (b) T142L, (c) T146A, (d) E361Q, (e) N372D, (f) N372S.

solvated environment offering flexibility to the macromolecules and therefore providing data with utmost biological relevance (Hospital et al., 2015; McCammon et al., 1977; Sharma et al., 2007). Therefore, in the present study molecular dynamics simulation was performed for the native unbound, substrate fumarate bound and inhibitor citrate bound complexes of zebrafish fumarate hydratase to further confirm the binding affinity of the substrate fumarate and inhibitor citrate.

The RMSD of the backbone atoms (unbound complex, fh-fumarate complex and fh-citrate complex) from the 30 ns trajectory showed that all the three complexes converged beyond 10 ns with the RMSD within 0.7 nm (Figure 6(a)). While no major difference was observed in the RMSD between unbound and fumarate bound complexes, the inhibitor citrate bound complex showed nearly 0.2 nm difference in its RMSD with that of the substrate. This indicates that the citrate binding influences the structure of the protein. A similar observation was obtained when molecular dynamics analysis of citrate bound FH complex was performed in the study by Subasri et al. (2017) which showed that the deviation in the structure of bound complex was in the acceptable limit, suggesting that binding of citrate did not alter the dynamic equilibrium of the FH protein structure (Subasri et al., 2017). This observation suggests that citrate can bind competitively to fumarate and inhibit the function of protein with maximum efficacy.

Root mean square fluctuation (RMSF)

The root mean square fluctuation (RMSF) for all the three structures predicted across all trajectory frames is displayed in Figure 6b. In all three structures the terminal ends show larger fluctuations since the terminal region is prone to vibrate (Subasri et al., 2017). Larger fluctuations observed within the internal regions were due to the loop regions within the protein. Comparatively we noted that the fumarate and unbound complexes exhibited minimal fluctuations than that of inhibitor citrate, indicating a more compact structure of the protein fh, while the citrate binding has imposed a conformational flexibility within the protein but to a lesser extent. In all the three structures the N-terminal ends remained unaltered, indicating the substrate and inhibitor binding influences the residues downstream of the binding cavity. While our observations from RMSD and RMSF lead to the speculation that the citrate binding have a larger influence on the protein than its substrate fumarate, in human FH analysis, citrate was found to be in a steady state with an RMSF value of 2.0 Å (Subasri et al., 2017). This suggests that citrate has more potential inhibitory effect on zebrafish fh when compared to human FH.

Intermolecular interactions between receptor and ligands

The intermolecular interactions of the substrate fumarate and inhibitor citrate with the protein were calculated in terms of the hydrogen bonds as a function of time and shown in Figure. 7. The results appear contrary to the interactions observed in the static mode of the protein shown in Figure. 2. This justifies the need to study the protein in a solvent guided environment where the conformational dynamics of proteins and ligands alters its behaviour in a realistic system. The hydrogen bonds results obtained from

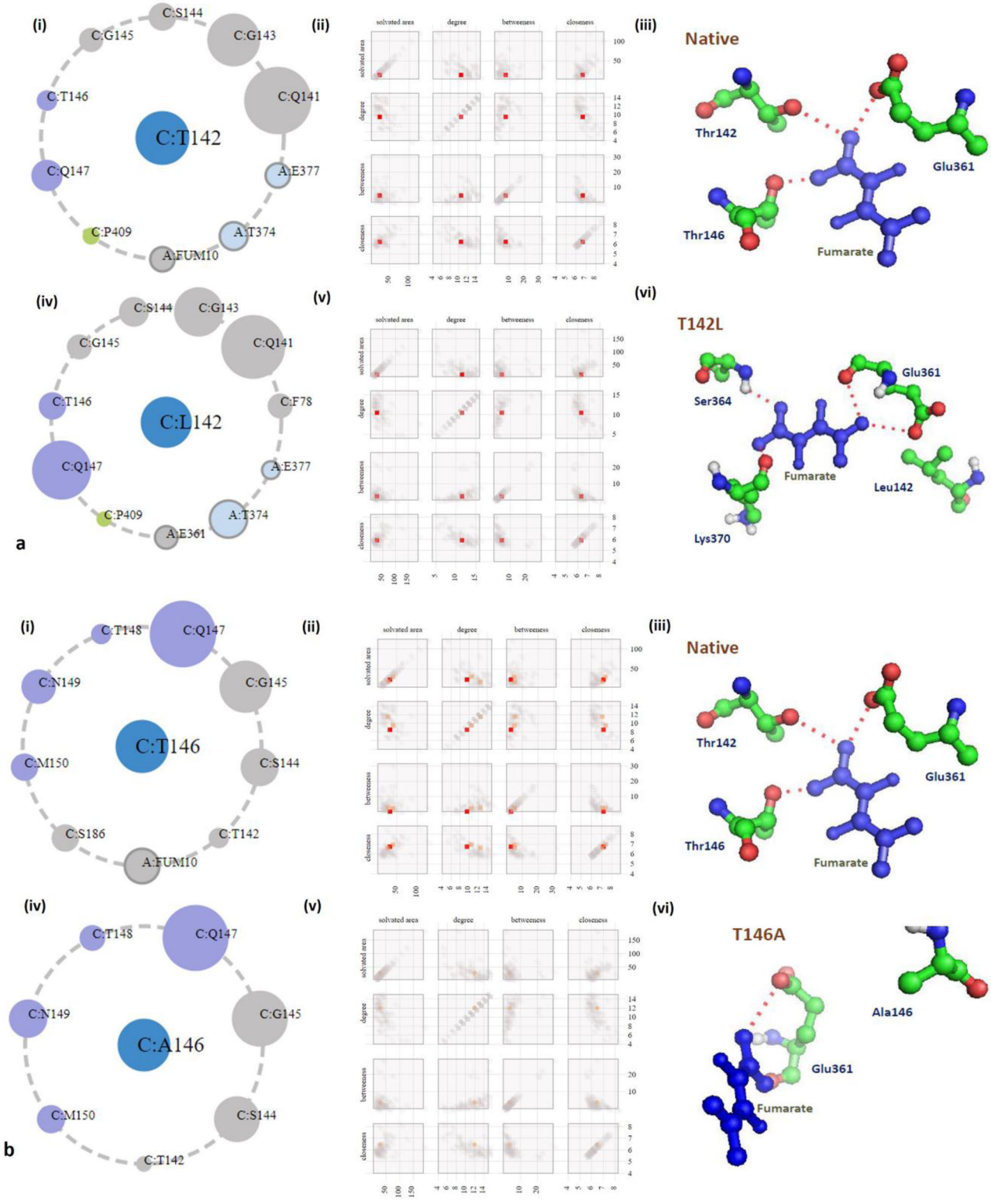

Figure 5. Interaction of ligand fumarate with active site residues in their native and mutated forms, (a) T142L, (b) T146A, (c) E361Q, (d) N372D, (e) N372S. Asteroid plot showing the interaction between the active site residue and their interacting residues, the native (a-d (i)) and the corresponding mutated (a-d (iv) and e (i)) active site residue is placed in the center (coloured in blue) and the interacting residues are shown in the nodes (different size of the node indicates the number of atomic contact the residue is having with the corresponding active site residue).

the trajectory frames corroborate the RMSD and RMSF speculations, in that the citrate shows a minimum of 6 and a maximum of 9 bonds with the fh in most of the frames. On the contrary, fumarate shuttles between 2 and 7 intermolecular hydrogen bonds. This further confirms that citrate has a stronger binding affinity than fumarate.

However, fluctuations in the number of hydrogen bonds are observed across the trajectory and therefore the

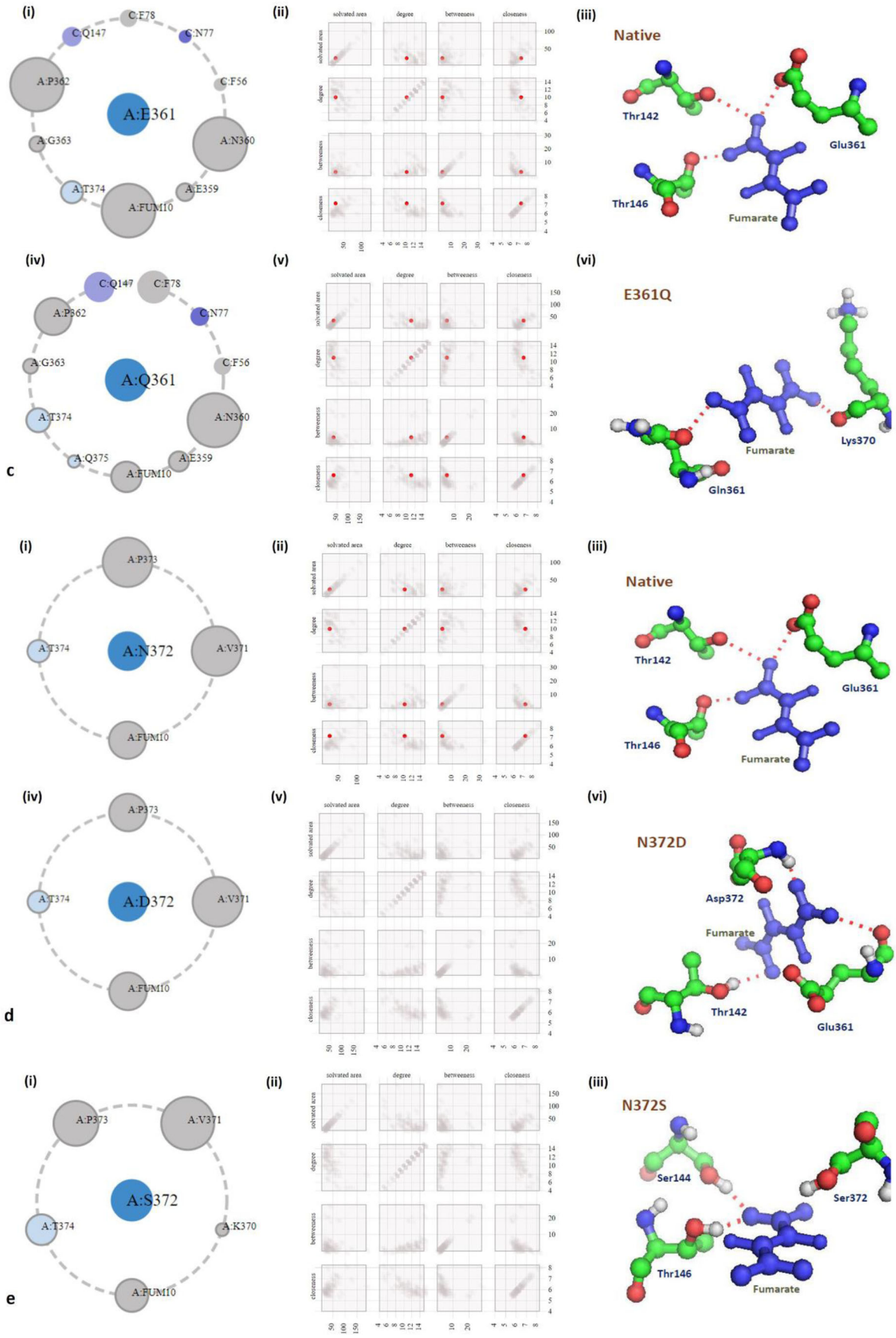

Figure 5. Continued.

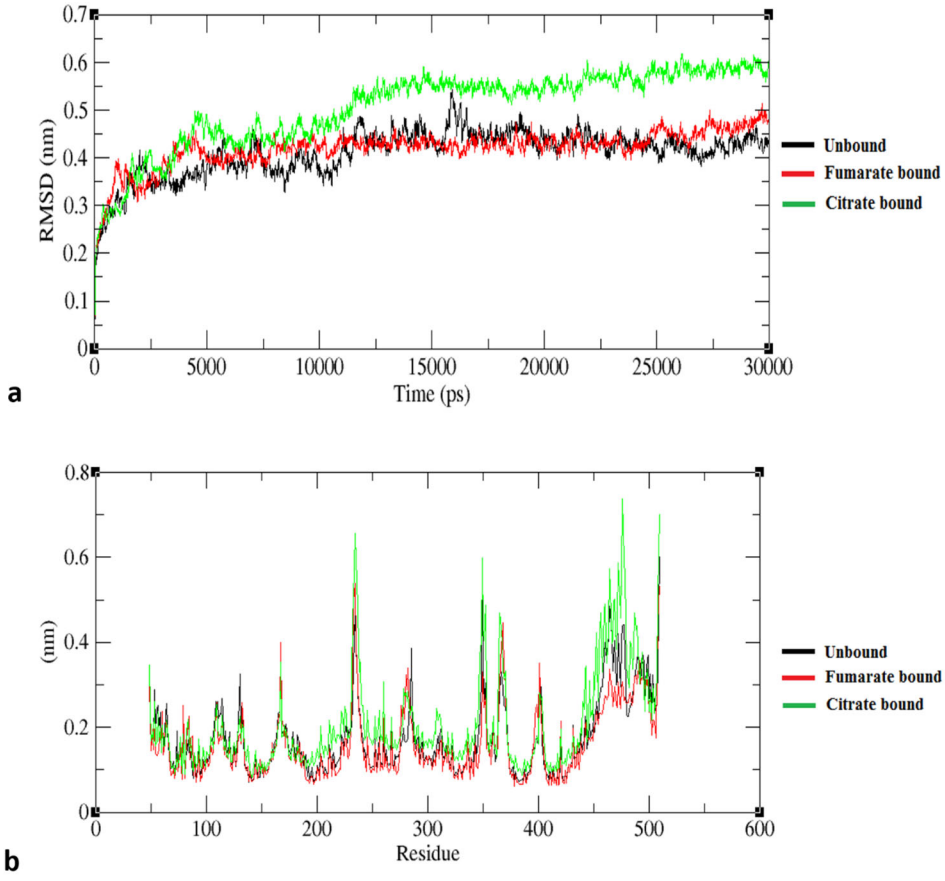

Figure 6. (a) Root Mean Square Deviation (RMSD), (b) Root Mean Square Fluctuation (RMSF) of native (unbound), fumarate bound and citrate bound to fumarate hydratase.

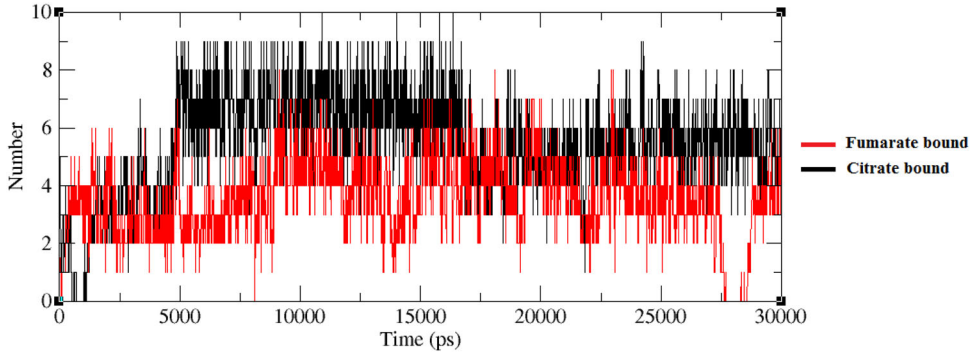

Figure 7. Number of hydrogen bonds of fumarate bound and citrate bound to fumarate hydratase.

Table 2. Hydrogen bond interaction between fh and substrate fumarate and inhibitor Citrate.

	% of residues showing hydrogen bond	
Residues	Citrate (%)	Fumarate
Ser186	108.53	129.91
Ser364	108.19	96.60
Ser365	66.06	9.43
Asn177	47.70	14.42
Asn181	27.42	2.90
Lys370	21.55	6.86
Asn187	18.72	2.86
Asn372	14.69	4.36
Ile366	10.43	–
Asn149	6.23	0.90
Thr146	3.53	1.73

persistence of these hydrogen bonds was predicted. About 30 bonds were observed in citrate complex and 22 bound with fumarate, among which 3 bonds in citrate and 2 bonds in fumarate were persistent in more than 50% of the trajectory frames as shown in Table 2. Both the ligands showed a strong bonded interaction with Ser186 and Ser364 with almost all the frames exhibiting interaction with these residues. Contrarily, both the ligands had very poor bonded interactions with the binding site residue Thr146 approximating to only 3-1% of the trajectory frames. Nevertheless, the residues bonded to the ligands were at closer proximity to the ligands and hence play a major role in holding the ligands intact at the binding site. About 11 residues

appeared to be common in both citrate and fumarate in bonding with the protein, however, the persistence of these residues to bond with the proteins was very less in fumarate in comparison with citrate as can be inferred from Table 2. From the table it is clear that the ligand binding to fumarate hydratase is highly dependent on the polar and charged residues namely serine, asparagine and lysine.

Interestingly, the corresponding residues Thr147, Thr146 and Thr100 of human FH, zebrafish fh and *E.coli* fh respectively were involved in the interaction with citrate although the interaction pattern was feeble hydrogen bonding (Human FH: Subasri et al., 2017; *E.coli* fh: Weaver et al., 1996). Apart from these residues, the other residues involved in the interaction of human FH and citrate were Glu148, Gln362, Pro363 and Asn373 (Subasri et al., 2017), while in *E.coli* the interacting residues were His188, Lys324, Asn326, Asn141, Asn135, Ser139, Ser140 and Thr100 (Weaver et al., 1996). Further, the docking analysis in our study showed that residue Gln361 of zebrafish fh forms hydrogen bond with citrate but in the simulation analysis, the behavior of the complex was found to be different where Gln361 residue of zebrafish fh was found to form a hydrophobic bond with citrate. However, the residue Ser139 of *E. coli* fh, which is the corresponding residue to Ser187 in zebrafish in our study, shows a strong hydrogen bond interaction with citrate (Weaver et al., 1996). These findings demonstrate that although the residues involved in hydrogen bond interactions are different in different species there are few crucial residues like threonine and serine which are conserved across the kingdom and found to play a vital role in establishing the fh-citrate interaction.

Contribution of residues towards protein ligand interactions

In order to predict the energetics of the protein-ligand interactions we calculated the overall and individual energy contribution of the residues bound with the ligands. The binding energies were predicted using mmpbsa method implemented in Gromacs and are listed in Table. 3. As expected from previous analysis, citrate showed a higher binding affinity with −115.979 kcal/mol, with fumarate as low as −75.655 kcal/mol. Since the intermolecular hydrogen bond interaction was largely guided by polar and charged residues, the difference in the binding energies of citrate and fumarate largely differed in electrostatic energy as observed in the table. The increase in the polar salvation energy of citrate justifies the difference in the fluctuation of the residues observed through the RMSF plot. The individual energy contribution of the residues indicates a very stable molecular mechanical energy in citrate, thus ensures the firm binding of the citrate within the receptor which corroborates with the minimal RMSD of the ligand. The individual energy contributions of the hydrogen bonded residues showed that the residues Ser186 had only a marginal difference in their binding energy between citrate and fumarate as shown in Table. 4. In contrast, the residues Ser364 and Ser365 which appeared to be bonded in more than 50% of the citrate and fumarate trajectory frames, contributed very less to the overall binding energy score as seen in the table. Comparing all the residues we noted that Asn149, Asn177 and Asn187 together contribute largely to the binding energy score, whereas in *E.coli*, Asn141 residue was found to be involved in the hydrogen bond interaction between fh and citrate, suggesting that asparagine is one of the important residues involved in the interaction of citrate with fh (Weaver et al., 1996).

Consolidating the overall analysis of docking and simulation it can be concluded that citrate has a higher and stable binding affinity towards fumarate and therefore can be used as inhibitor of fumarate hydratase.

Table 3. Calculated binding energy for fh with substrate fumarate and inhibitor citrate.

Energy terms (in kcal/mol)	Citrate	Fumarate
van der Waal energy	−17.316	−13.530
Electrostatic energy	−688.930	−435.901
Polar solvation energy	598.614	379.416
SASA energy	−8.347	−5.641
SAV energy	–	–
WCA energy	–	–
Binding energy	−115.979	−75.655

Analysis of inhibition of zebrafish fh activity by citrate

In order to confirm the above findings an *in vitro* analysis of fumarate hydratase activity with inhibitor citrate was performed using zebrafish tissue homogenate. As observed in the *in-silico* analysis the results showed a reduced fh activity in a concentration specific manner. In this experiment the group treated with 5 mM and 10 mM citrate showed a decrease in fh activity in a concentration dependent manner

Table 4. Energy contribution of residues towards ligand binding.

	MM (in kcal/mol)		Polar (in kcal/mol)		APolar (in kcal/mol)		Total (in kcal/mol)	
Residues	Fumarate	Citrate	Fumarate	Citrate	Fumarate	Citrate	Fumarate	Citrate
Thr-146	−1.5137	−4.7752	1.0623	2.8641	−0.0276	−0.0968	−0.5051	−1.9954
Asn-149	−9.5949	−13.9806	7.4686	9.9659	−0.0322	−0.0681	−2.1608	−4.1179
Asn-177	−5.9645	−17.2642	6.3791	17.5018	−0.1666	−0.4722	0.2222	−0.2641
Asn-181	−1.4334	−6.7107	1.424	5.9233	−0.0705	−0.0788	−0.05	−0.9109
Ser-186	−31.8699	−33.5663	29.2372	30.4943	−0.3922	−0.6606	−2.9754	−3.7747
Asn-187	−11.9118	−19.6858	10.3301	15.8319	−0.1616	−0.2078	−1.6551	−4.0632
Ser-364	0.0105	0.0224	−0.0018	−0.003	0	0	0.0087	0.0185
Ser-365	−0.0032	0.0407	−0.0009	−0.0021	0	0	−0.0038	0.0387
Ile-366	0.0313	−0.0518	−0.0032	0.0013	0	0	0.0278	−0.0506
Lys-370	−11.169	−16.4097	0.0345	0.0254	0	0	−11.1351	−16.3822
Asn-372	−0.108	0.045	0.0106	−0.0037	0	0	−0.0972	0.0418
Total	−73.5266	−112.336	55.9405	82.5992	−0.8507	−1.5843	−18.3238	−31.46

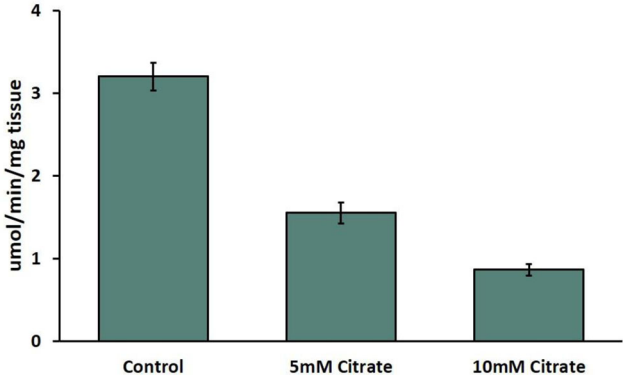

Figure 8. Concentration dependent inhibition of zebrafish fumarate hydratase enzyme activity by citrate.

as shown in Figure 8. This explains a concentration dependent inhibition of fumarate hydratase activity by inhibitor citrate.

Conclusion

The modelled zebrafish native fh structure has been docked with its substrate fumarate and inhibitor citrate in the active site of zebrafish fumarate hydratase. This led to the identification of interacting residues of zebrafish fh to fumarate and citrate and the subsequent analysis of these residues were found to be critical, as mutation in these residues lead to a negative impact on protein structure which drastically altered its binding efficacy with its substrate. In addition, docking of substrate fumarate with a mutant fh also showed altered molecular interactions with the ligand. Comparison of binding affinities obtained from the substrate and inhibitor suggests that the inhibitor can prevent binding of the substrate fumarate to the fh active site. Further molecular simulation analysis together with *in vitro* fumarate hydratase activity assay also confirms these findings. It is therefore suggested that the inhibitor citrate can be used in zebrafish to mimic some of the fumarate hydratase dysfunction conditions in human.

Acknowledgements

The authors would also like to thank SRMIST for the facilities for carrying out the experiments. The authors of the article would like to thank DST-SERB, Government of India for the funding (grant no. YSS/2014/000017).

Disclosure statement

No potential conflict of interest was reported by the author(s).

References

Adzhubei, I. A., Schmidt, S., Peshkin, L., Ramensky, V. E., Gerasimova, A., Bork, P., Kondrashov, A. S., & Sunyaev, S. R. (2010). A method and server for predicting damaging missense mutations. *Nature Methods*, *7*(4), 248–249. https://doi.org/10.1038/nmeth0410-248

Alam, N. A., Olpin, S., Rowan, A., Kelsell, D., Leigh, I. M., Tomlinson, I. P., & Weaver, T. (2005). Missense mutations in fumarate hydratase in multiple cutaneous and uterine leiomyomatosis and renal cell cancer. *The Journal of Molecular Diagnostics*, *7*(4), 437–443. https://doi.org/10.1016/S1525-1578(10)60574-0

Ashkenazy, H., Abadi, S., Martz, E., Chay, O., Mayrose, I., Pupko, T., & Ben-Tal, N. (2016). ConSurf 2016: an improved methodology to estimate and visualize evolutionary conservation in macromolecules. *Nucleic Acids Research*, *44*(W1), W344–W350. https://doi.org/10.1093/nar/gkw408

Berendsen, H., Van Der Spoel, D., & Van Drunen, R. (1995). GROMACS: A message-passing parallel molecular dynamics implementation. *Computer Physics Communications*, *91*(1-3), 43–56. https://doi.org/10.1016/0010-4655(95)00042-E

Bulku, A., Weaver, T. M., & Berkmen, M. B. (2018). Biochemical characterization of two clinically-relevant human fumarase variants defective for oligomerization. *The Open Biochemistry Journal*, *12*(1), 1–15. https://doi.org/10.2174/1874091X01812010001

Capriotti, E., Calabrese, R., Fariselli, P., Martelli, P., Altman, R. B., & Casadio, R. (2013). WS-SNPs&GO: a web server for predicting the deleterious effect of human protein variants using functional annotation. *BMC Genomics*., *14*(Suppl 3), S6. https://doi.org/10.1186/1471-2164-14-S3-S6

Castro-Vega, L. J., Buffet, A., De Cubas, A. A., Cascón, A., Menara, M., Khalifa, E., … Gimenez-Roqueplo, A. P. (2014). Germline mutations in FH confer predisposition to malignant pheochromocytomas and paragangliomas. *Human Molecular Genetics*, *23*(9), 2440–2446. https://doi.org/10.1093/hmg/ddt639

Choi, Y., & Chan, A. P. (2015). PROVEAN web server: a tool to predict the functional effect of amino acid substitutions and indels. *Bioinformatics*, *31*(16), 2745–2747. https://doi.org/10.1093/bioinformatics/btv195

Doonan, S., Barra, D., & Bossa, F. (1984). Structural and genetic relationships between cytosolic and mitochondrial isoenzymes. *The International Journal of Biochemistry*, *16*(12), 1193–1199. https://doi.org/10.1016/0020-711X(84)90216-7

Guex, N., & Peitsch, M. C. (1997). SWISS-MODEL and the Swiss-Pdb Viewer: An environment for comparative protein modeling. *Electrophoresis*, *18*(15), 2714–2723. https://doi.org/10.1002/elps.1150181505

Hospital, A., Goñi, J. R., Orozco, M., & Gelpí, J. L. (2015). Molecular dynamics simulations: Advances and applications. *Advances and Applications in Bioinformatics and Chemistry*, *8*, 37–47.

Isaacs, J. S., Jung, Y. J., Mole, D. R., Lee, S., Torres-Cabala, C., Chung, Y. L., … Neckers, L. (2005). HIF overexpression correlates with biallelic loss of fumarate hydratase in renal cancer: Novel role of fumarate in regulation of HIF stability. *Cancer Cell*, *8*(2), 143–153. https://doi.org/10.1016/j.ccr.2005.06.017

Jiang, Y., Qian, X., Shen, J., Wang, Y., Li, X., Liu, R., … Lu, Z. (2015). Local generation of fumarate promotes DNA repair through inhibition of histone H3 demethylation. *Nature Cell Biology*, *17*(9), 1158–1168. https://doi.org/10.1038/ncb3209

Kayikci, M., Venkatakrishnan, A. J., Scott-Brown, J., Ravarani, C., Flock, T., & Babu, M. M. (2018). Visualization and analysis of non-covalent contacts using the protein contacts atlas. *Nature Structural & Molecular Biology*, *25*(2), 185–194. https://doi.org/10.1038/s41594-017-0019-z

Laskowski, R. A., & Swindells, M. B. (2011). LigPlot+: Multiple Ligand–Protein Interaction Diagrams for Drug Discovery. *Journal of Chemical Information and Modeling*, *51*(10), 2778–2786. https://doi.org/10.1021/ci200227u

Leshets, M., Silas, Y., Lehming, N., & Pines, O. (2018). Fumarase: From the TCA cycle to DNA damage response and tumour suppression. *Frontiers in Molecular Biosciences*, *5*, 68–77. https://doi.org/10.3389/fmolb.2018.00068

Mann, P. J., & Woolf, B. (1930). The action of salts on fumarase. I. .*The Biochemical Journal*, *24*(2), 427–434. https://doi.org/10.1042/bj0240427

McCammon, J. A., Gelin, B. R., & Karplus, M. (1977). Dynamics of folded proteins. *Nature*, *267*(5612), 585–590. https://doi.org/10.1038/267585a0

Mi, H., Dong, Q., Muruganujan, A., Gaudet, P., Lewis, S., & Thomas, P. D. (2010). PANTHER version 7: improved phylogenetic trees, orthologs and collaboration with the Gene Ontology Consortium. *Nucleic Acids*

Research, *38*(suppl_1), D204–D210. https://doi.org/10.1093/nar/gkp1019

O'Hare, M. C., & Doonan, S. (1985). Purification and structural comparisons of the cytosolic and mitochondrial isoenzymes of fumarase from pig liver. *Biochimica et Biophysica Acta (BBA) – Protein Structure and Molecular Enzymology*, *827*(2), 127–134.

Patel, M., Day, B. J., Crapo, J. D., Fridovich, I., & McNamara, J. O. (1996). Requirement for superoxide in excitotoxic cell death. *Neuron*, *16*(2), 345–355. https://doi.org/10.1016/S0896-6273(00)80052-5

Picaud, S., Kavanagh, K. L., Yue, W. W., Lee, W. H., Muller-Knapp, S., Gileadi, O., Sacchettini, J., & Oppermann, U. (2011). Structural basis of fumarate hydratase deficiency. *Journal of Inherited Metabolic Disease*, *34*(3), 671–676. https://doi.org/10.1007/s10545-011-9294-8

Pollard, P. J., Brière, J. J., Alam, N. A., Barwell, J., Barclay, E., Wortham, N. C., Hunt, T., Mitchell, M., Olpin, S., Moat, S. J., Hargreaves, I. P., Heales, S. J., Chung, Y. L., Griffiths, J. R., Dalgleish, A., McGrath, J. A., Gleeson, M. J., Hodgson, S. V., Poulsom, R., Rustin, P., & Tomlinson, I. P. M. (2005). Accumulation of Krebs cycle intermediates and overexpression of HIF1alpha in tumours which result from germline FH and SDH mutations. *Human Molecular Genetics*, *14*(15), 2231–2239. https://doi.org/10.1093/hmg/ddi227

Schmidt, C., Sciacovelli, M., & Frezza, C. (2020). Fumarate hydratase in cancer: A multifaceted tumour suppressor. *Seminars in Cell & Developmental Biology*, *98*, 15–25. https://doi.org/10.1016/j.semcdb.2019.05.002

Schneidman-Duhovny, D., Inbar, Y., Nussinov, R., & Wolfson, H. J. (2005). PatchDock and SymmDock: servers for rigid and symmetric docking. *Nucleic Acids Research*, *33*, W363–W367. https://doi.org/10.1093/nar/gki481

Sharma, S., Ding, F., & Dokholyan, N. V. (2007). Multiscale modeling of nucleosome dynamics. *Biophysical Journal*, *92*(5), 1457–1470. https://doi.org/10.1529/biophysj.106.094805

Sim, N.-L., Kumar, P., Hu, J., Henikoff, S., Schneider, G., & Ng, P. C. (2012). SIFT web server: predicting effects of amino acid substitutions on proteins. *Nucleic Acids Research*, *40*(W1), W452–W457. https://doi.org/10.1093/nar/gks539

Subasri, S., Chaudhary, S. K., Sekar, K., Kesherwani, M., & Velmurugan, D. (2017). Molecular docking and molecular dynamics simulations of fumarate hydratase and its mutant H235N complexed with pyromellitic acid and citrate. *Journal of Bioinformatics and Computational Biology*, *15*(6), 1750026. https://doi.org/10.1142/S0219720017500263

Teipel, J. W., & Hill, R. L. (1968). The number of substrate- and inhibitor-binding sites of fumarase. *The Journal of Biological Chemistry*, *243*(21), 5679–5683.

Tomlinson, I. P., Alam, N. A., Rowan, A. J., Barclay, E., Jaeger, E. E., Kelsell, D, … Multiple Leiomyoma Consortium 20. (2002). Germline mutations in FH predispose to dominantly inherited uterine fibroids, skin leiomyomata and papillary renal cell cancer. *Nature Genetics*, *30*(4), 406–410.

Trpkov, K., Hes, O., Agaimy, A., Bonert, M., Martinek, P., Magi-Galluzzi, C., … Gill, A. J. (2016). Fumarate Hydratase-deficient renal cell carcinoma is strongly correlated with fumarate hydratase mutation and hereditary leiomyomatosis and renal cell carcinoma syndrome. *The American Journal of Surgical Pathology*, *40*(7), 865–875.

Weaver, T., & Banaszak, L. (1996). Crystallographic studies of the catalytic and a second site in fumarase C from Escherichia coli. *Biochemistry*, *35*(44), 13955–13965. https://doi.org/10.1021/bi9614702

Webb, B., & Sali, A. (2016). Comparative Protein Structure Modeling Using MODELLER. *Current Protocols in Bioinformatics*, *54*(1). https://doi.org/10.1002/cpbi.3

Woods, S. A., Schwartzbach, S. D., & Guest, J. R. (1988). Two biochemically distinct classes of fumarase in Escherichia coli. *Biochimica et Biophysica Acta (Bba) – Protein Structure and Molecular Enzymology*, *954*(1), 14–26. https://doi.org/10.1016/0167-4838(88)90050-7

Wu, M., & Tzagoloff, A. (1987). Mitochondrial and cytoplasmic fumarases in Saccharomyces cerevisiae are encoded by a single nuclear gene FUM1. *The Journal of Biological Chemistry*, *262*(25), 12275–12282.

Yogev, O., Yogev, O., Singer, E., Shaulian, E., Goldberg, M., Fox, T. D., & Pines, O. (2010). Fumarase: A mitochondrial metabolic enzyme and a cytosolic/nuclear component of the DNA damage response. *PLoS Biology*, *8*(3), e1000328. https://doi.org/10.1371/journal.pbio.1000328